Kalman's Shrinkage for Wavelet-Based Despeckling of SAR Images

Mario Mastriani, and Alberto E. Giraldez

Abstract—In this paper, a new probability density function (pdf) is proposed to model the statistics of wavelet coefficients, and a simple Kalman's filter is derived from the new pdf using Bayesian estimation theory. Specifically, we decompose the speckled image into wavelet subbands, we apply the Kalman's filter to the high subbands, and reconstruct a despeckled image from the modified detail coefficients. Experimental results demonstrate that our method compares favorably to several other despeckling methods on test synthetic aperture radar (SAR) images.

Keywords—Kalman's filter, shrinkage, speckle, wavelets.

I. INTRODUCTION

THE despeckling of a SAR image corrupted by speckle noise is an important problem in image processing. If the wavelet transform and maximum a-posteriori (MAP) estimator are used for this problem, the solution requires a priori knowledge about wavelet coefficients. Therefore, two problems arise: 1) What kind of distribution represents the wavelet coefficients? 2) What is the corresponding estimator (shrinkage function) ?

Statistical models pretend wavelet coefficients to be random realizations from a distribution function. For the first problem, mostly these models assume the coefficients are time-invariant, and try to characterize them by using Gaussian, Laplacian, or Gaussian scale mixtures. For example, classical soft thresholding operator suggested by Donoho [1] can be obtained by a Laplacian assumption. Bayesian methods for image denosing using other distributions have also been proposed [2]–[6].

The wavelet transform has become an important tool for this problem due to its energy compaction property. Basically, it states that the wavelet transform yields a large number of small coefficients and a small number of large coefficients.

Simple denoising algorithms that use the wavelet transform consist of three steps:

1) Calculate the wavelet transform of the noisy image.
2) Modify the noisy wavelet coefficients according to some rule.

3) Compute the inverse transform using the modified coefficients.

Besides, two properties are very important for the following deduction: 1) If a wavelet coefficient is large/small, the adjacent coefficients are likely to be large/small, and 2) large/small coefficients tend to propagate across the scales [7]-[9]. In this paper, we use a new time-variant pdf and derive a Kalmanian shrinkage (KalmanShrink) function using Bayesian estimation theory.

II. BAYESIAN DENOISING

In this section, the denoising of an image corrupted by white Gaussian noise will be considered, i.e.,

$$g = x + n \qquad (1)$$

where n is independent Gaussian noise. We observe g (a noisy signal) and wish to estimate the desired signal x as accurately as possible according to some criteria. In the wavelet domain, if we use an orthogonal wavelet transform, the problem can be formulated as

$$y = w + n \qquad (2)$$

where y noisy wavelet coefficient, w true coefficient, and n noise, which is independent Gaussian. This is a classical problem in estimation theory. Our aim is to estimate from the noisy observation. The MAP estimator will be used for this purpose. Time-variant and time-invariant models will be discussed for this problem in Sections II-A and B, and new MAP estimators are derived.

A. Time-Invariant Models

The classical MAP estimator for (2) is

$$\hat{w}(y) = \arg \max_{w} p_{w|y}(w \mid y). \qquad (3)$$

Using Bayes rule, one gets

$$\hat{w}(y) = \arg \max_{w} \left[p_{y|w}(y \mid w) \cdot p_{w}(w) \right]$$

$$= \arg \max_{w} \left[p_{n}(y - w) \cdot p_{w}(w) \right]. \qquad (4)$$

Therefore, these equations allow us to write this estimation in terms of the pdf of the noise (p_n) and the pdf of the signal coefficient (p_w). From the assumption on the noise, p_n is zero mean Gaussian with variance σ_n, i.e.,

$$p_n(n) = \frac{1}{\sigma_n \sqrt{2\pi}} . \exp\left(- \frac{n^2}{2\sigma_n^2} \right). \qquad (5)$$

It has been observed that wavelet coefficients of natural images have highly non-Gaussian statistics [7]-[9]. The pdf for wavelet coefficients is often modeled as a generalized (heavy-tailed) Gaussian [7]-[9].

$$p_w(w) = K(s,p) . \exp\left(- \left| \frac{w}{s} \right|^p \right). \qquad (6)$$

where s, p are the parameters for this model, and $K(s, p)$ is the parameter-dependent normalization constant. Other pdf models have also been proposed [7]-[9]. In practice, generally, two problems arise with the Bayesian approach when an accurate but complicated pdf $p_w(w)$ is used: 1) It can be difficult to estimate the parameters of p_w for a specific image, especially from noisy data, and 2) the estimators for these models may not have simple closed form solution and can be difficult to obtain. The solution for these problems usually requires numerical techniques.

Let us continue developing the MAP estimator and show it for Gaussian and Laplacian cases. Equation (4) is also equivalent to

$$\hat{w}(y) = \arg\max_{w} \left[\log(p_n(y - w) + \log(p_w(w)) \right]. \qquad (7)$$

As in [7]-[9], let us define $f(w) = \log(p_w(w))$. By using (5), (7) becomes

$$\hat{w}(y) = \arg\max_{w} \left[-\frac{(y-w)^2}{2\sigma_n^2} + f(w) \right]. \qquad (8)$$

This is equivalent to solving the following equation for $\hat{w}$ if $p_w(w)$ is assumed to be strictly convex and differentiable.

$$\frac{y - \hat{w}}{\sigma_n^2} + f'(\hat{w}) = 0. \qquad (9)$$

If $p_w(w)$ is assumed to be a zero mean gaussian density with variance σ^2, then $f(w) = -\log(\sqrt{2\pi}\sigma) - w^2/2\sigma^2$, and the estimator can be written as

$$\hat{w}(y) = \frac{\sigma^2}{\sigma^2 + \sigma_n^2} . y. \qquad (10)$$

If it is Laplacian

$$p_w(w) = \frac{1}{\sqrt{2}\sigma} \exp\left(- \frac{\sqrt{2}|w|}{\sigma} \right). \qquad (11)$$

then $f(w) = -\log(\sigma\sqrt{2}) - \sqrt{2}|w|/\sigma$, and the estimator will be

$$\hat{w}(y) = \operatorname{sign}(y) \left(|y| - \frac{\sqrt{2}\sigma_n^2}{\sigma} \right)_+ . \qquad (12)$$

Here, $(g)_+$ is defined as

$$(g)_+ = \begin{cases} 0, & \text{if } g < 0 \\ g, & \text{otherwise} \end{cases} \qquad (13)$$

Equation (12) is the classical soft shrinkage function. Let us define the soft operator as

$$\operatorname{soft}(g, \tau) = \operatorname{sign}(g) . (|g| - \tau)_+ . \qquad (14)$$

The soft shrinkage function (12) can be written as

$$\hat{w}(y) = \operatorname{soft}\left(y, \frac{\sqrt{2}\sigma_n^2}{\sigma} \right) . \qquad (15)$$

B. Time-Variant Model (KalmanShrink)

Time-invariant models cannot model the temporal variation of wavelet coefficients. However, the coefficients depend strongly on the time. This paper suggests such dependency and derives the corresponding Kalmanian MAP estimator based on noisy wavelet coefficients in detail.

Here, we modify the Bayesian estimation problem as to take into account the time dependency of coefficients. If pdf is

$$p_w(w) = \exp\left(- \frac{1}{\sigma_n^2 K_t} \sum_w (\hat{w}_{t+1}(y) - \hat{w}_t(y)) \right). \qquad (16)$$

then

$$f(\hat{w}) = -\frac{1}{\sigma_n^2 K_t} \sum_w (\hat{w}_{t+1}(y) - \hat{w}_t(y)). \qquad (17)$$

with

$$f'(\hat{w}) = -\frac{(\hat{w}_{t+1}(y) - \hat{w}_t(y))}{\sigma_n^2 K_t}. \tag{18}$$

Replacing (18) into (9), the estimator can be written as

$$\hat{w}_{t+1}(y) = \hat{w}_t(y) + K_t.(y_t - \hat{w}_t). \tag{19}$$

and

$$\hat{y}_t = \hat{w}_t(y). \tag{20}$$

where $\mathbf{K}_t$ is the Kalman's gain of the Kalman's filter [10]-[15], being

$$K_t = \frac{P_t}{P_t + \sigma_n^2} \tag{21}$$

and

$$P_t = (1 - K_t).P_t \tag{22}$$

is the norm of error covariance, that is to say

$$P_t = \left\| E\{(y_t - \hat{w}_t).(y_t - \hat{w}_t)^{\mathrm{T}}\} \right\|_2. \tag{23}$$

where $[\bullet]^{\mathrm{T}}$ means transpose of $[\bullet]$, $E\{\bullet\}$ means the expectation of $\{\bullet\}$ and $\|(\bullet)\|_2$ means the L_2-norm of $(\bullet)$. Finally, the original system is formed by (2) and

$$w_{t+1} = w_t. \tag{24}$$

These equations can be described as a Kalman filter loop [10] as follows:

1) Calculate σ_n^2 as the variance of (2)

2) Initialize $\hat{w}$ and P

3) Choose P_{final} as a finish condition

4) *while* $\mathrm{P}_t > \mathrm{P}_{final}$,

   Compute Kalman's gain K_t from (21)

   Update estimate $\hat{w}_{t+1}(y)$ with measurement y_t from (19)

   Compute error covariance P_t for updated estimate from (22)

   end while.

III. Speckle Model

Speckle noise in SAR images is usually modeled as a purely multiplicative noise process of the form

$$I_s(r,c) = I(r,c).S(r,c)$$

$$= I(r,c).[1 + S'(r,c)]$$

$$= I(r,c) + N(r,c) \tag{25}$$

The true radiometric values of the image are represented by I, and the values measured by the radar instrument are represented by I_s. The speckle noise is represented by S. The parameters r and c means row and column of the respective pixel of the image. If

$$S'(r,c) = S(r,c) - 1 \tag{26}$$

and

$$N(r,c) = I(r,c).S'(r,c) \tag{27}$$

we begin with a multiplicative speckle S and finish with an additive speckle N [16], which avoid the log-transform, because the mean of log-transformed speckle noise does not equal to zero [17] and thus requires correction to avoid extra distortion in the restored image.

For single-look SAR images, S is Rayleigh distributed (for amplitude images) or negative exponentially distributed (for intensity images) with a mean of 1. For multi-look SAR images with independent looks, S has a gamma distribution with a mean of 1. Further details on this noise model are given in [18].

IV. Assessment Parameters

In this work, the assessment parameters that are used to evaluate the performance of speckle reduction are Noise Variance, Mean Square Difference, Noise Mean Value, Noise Standard Deviation, Equivalent Number of Looks, Deflection Ratio [19], [20], and Pratt's figure of Merit [21].

A. Noise Mean Value (NMV), Noise Variance (NV), and Noise Standard Deviation (NSD)

NV determines the contents of the speckle in the image. A lower variance gives a "cleaner" image as more speckle is reduced, although, it not necessarily depends on the intensity. The formulas for the *NMV*, *NV* and *NSD* calculation are

$$NMV = \frac{\sum_{r,c} I_d(r,c)}{R * C} \tag{28.1}$$

$$NV = \frac{\sum_{r,c} (I_d(r,c) - NMV)^2}{R * C} \tag{28.2}$$

$$NSD = \sqrt{NV} \qquad (28.3)$$

where R-by-C pixels is the size of the despeckled image I_d. On the other hand, the estimated noise variance is used to determine the amount of smoothing needed for each case for all filters.

B. Mean Square Difference (MSD)

MSD indicates average square difference of the pixels throughout the image between the original image (with speckle) I_s and I_d, see Fig. 1. A lower *MSD* indicates a smaller difference between the original (with speckle) and despeckled image. This means that there is a significant filter performance. Nevertheless, it is necessary to be very careful with the edges. The formula for the *MSD* calculation is

$$MSD = \frac{\sum_{r,c}(I_s(r,c) - I_d(r,c))^2}{R * C} \qquad (29)$$

C. Equivalent Numbers of Looks (ENL)

Another good approach of estimating the speckle noise level in a SAR image is to measure the *ENL* over a uniform image region [20]. A larger value of *ENL* usually corresponds to a better quantitative performance. The value of *ENL* also depends on the size of the tested region, theoretically a larger region will produces a higher *ENL* value than over a smaller region but it also tradeoff the accuracy of the readings. Due to the difficulty in identifying uniform areas in the image, we proposed to divide the image into smaller areas of 25x25 pixels, obtain the *ENL* for each of these smaller areas and finally take the average of these *ENL* values. The formula for the *ENL* calculation is

$$ENL = \frac{NMV^2}{NSD^2} \qquad (30)$$

The significance of obtaining both *MSD* and *ENL* measurements in this work is to analyze the performance of the filter on the overall region as well as in smaller uniform regions.

D. Deflection Ratio (DR)

A fourth performance estimator that we used in this work is the *DR* proposed by H. Guo et al (1994), [22]. The formula for the deflection calculation is

$$DR = \frac{1}{R * C}\sum_{r,c}\left(\frac{I_d(r,c) - NMV}{NSD}\right) \qquad (31)$$

The ratio *DR* should be higher at pixels with stronger reflector points and lower elsewhere. In H. Guo *et al*'s paper, this ratio is used to measure the performance between different wavelet shrinkage techniques. In this paper, we apply the ratio approach to all techniques after despeckling in the same way [19].

E. Pratt's figure of merit (FOM)

To compare edge preservation performances of different speckle reduction schemes, we adopt the Pratt's figure of merit [21] defined by

$$FOM = \frac{1}{max\{\hat{N}, N_{ideal}\}}\sum_{i=1}^{\hat{N}}\frac{1}{1 + d_i^2\alpha} \qquad (32)$$

Where $\hat{N}$ and N_{ideal} are the number of detected and ideal edge pixels, respectively, d_i is the Euclidean distance between the ith detected edge pixel and the nearest ideal edge pixel, and α is a constant typically set to 1/9. *FOM* ranges between *0* and *1*, with unity for ideal edge detection.

V. EXPERIMENTAL RESULTS

Here, we present a set of experimental results using one ERS SAR Precision Image (PRI) standard of Buenos Aires area. For statistical filters employed along, i.e., Median, Lee, Kuan, Gamma-Map, Enhanced Lee, Frost, Enhanced Frost [19], [20], Wiener [23], DS [21] and Enhanced DS (EDS) [19], we use a homomorphic speckle reduction scheme [19], with 3-by-3, 5-by-5 and 7-by-7 kernel windows. Besides, for Lee, Enhanced Lee, Kuan, Gamma-Map, Frost and Enhanced Frost filters the damping factor is set to 1 [19], [20].

Fig. 1 shows a noisy image used in the experiment from remote sensing satellite ERS-2, with a 242-by-242 (pixels) by 65536 (gray levels); and the filtered images, processed by using VisuShrink (Hard-Thresholding), BayesShrink, NormalShrink, SUREShrink, and KalmanShrink techniques respectively, see Table I. All the wavelet-based techniques used Daubechies 1 wavelet basis and 1 level of decomposition (improvements were not noticed with other basis of wavelets) [4], [21], [23]. Besides, Fig. 1 summarizes the edge preservation performance of the KalmanShrink technique vs. the rest of the shrinkage techniques with a considerably acceptable computational complexity.

Table I shows the assessment parameters vs. 19 filters for Fig. 1, where En-Lee means Enhanced Lee Filter, En-Frost means Enhanced Frost Filter, Non-log SWT means Non-logarithmic Stationary Wavelet Transform Shrinkage [16], Non-log DWT means Non-logarithmic DWT Shrinkage [17], VisuShrink (HT) means Hard-Thresholding, (ST) means Soft-Thresholding, and (SST) means Semi-ST [4], [20], [22]-[28].

We compute and compare the NMV and NSD over six different homogeneous regions in our SAR image, before and after filtering, for all filters. The KalmanAShrink has obtained the best mean preservation and variance reduction, as shown

in Table I. Since a successful speckle reducing filter will not significantly affect the mean intensity within a homogeneous region, KalmanShrink demonstrated to be the best in this sense too. The quantitative results of Table I show that the KalmanShrink tech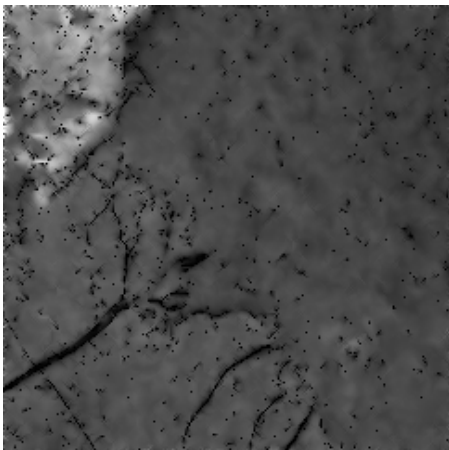nique can eliminate speckle without distorting useful image information and without destroying the important image edges. In fact, the KalmanShrink outperformed the conventional and no conventional speckle reducing filters in terms of edge preservation measured by
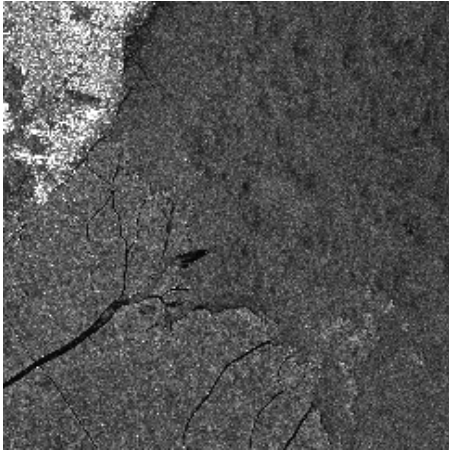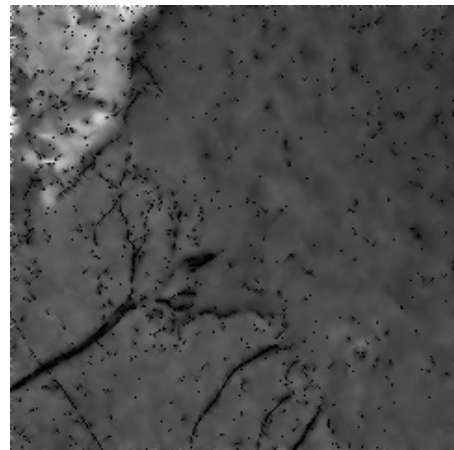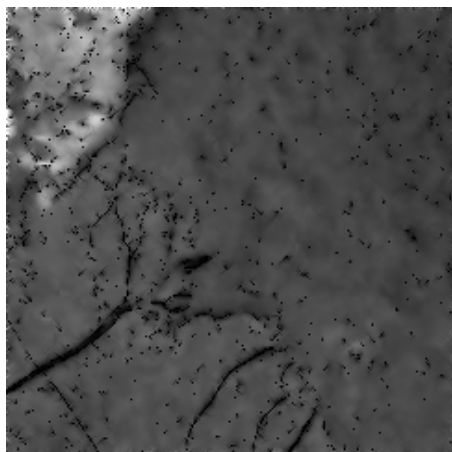

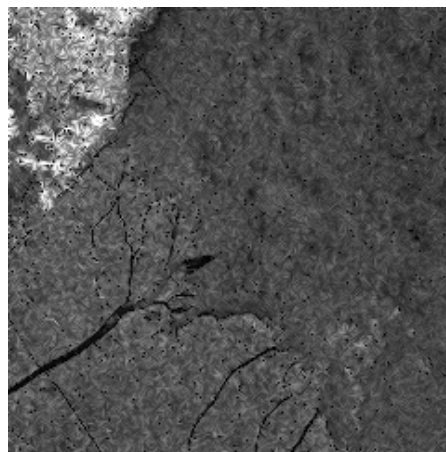(a) original
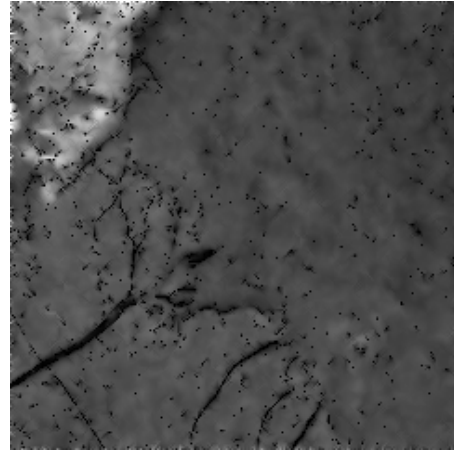
(b) VisuShrink

(c) BayesShrink

(d) NormalShrink

(e) SUREShrink

(f) KalmanShrink

Fig. 1 Original and filtered images

TABLE I
ASSESSMENT PARAMETERS VS. FILTERS FOR FIG. 1

Filter	Assessment Parameters					
	MSD	NMV	NSD	ENL	DR	FOM
Original noisy image	-	90.0890	43.9961	11.0934	2.5580e-017	0.3027
En-Frost	564.8346	87.3245	40.0094	16.3454	4.8543e-017	0.4213
En-Lee	532.0006	87.7465	40.4231	16.8675	4.4236e-017	0.4112
Frost	543.9347	87.6463	40.8645	16.5331	3.8645e-017	0.4213
Lee	585.8373	87.8474	40.7465	16.8465	3.8354e-017	0.4228
Gamma-MAP	532.9236	87.8444	40.6453	16.7346	3.9243e-017	0.4312
Kuan	542.7342	87.8221	40.8363	16.9623	3.2675e-017	0.4217
Median	614.7464	85.0890	42.5373	16.7464	2.5676e-017	0.4004
Wiener	564.8346	89.8475	40.3744	16.5252	3.2345e-017	0.4423
DS	564.8346	89.5353	40.0094	17.8378	8.5942e-017	0.4572
EDS	564.8346	89.3232	40.0094	17.4242	8.9868e-017	0.4573
VisuShrink (HT)	855.3030	88.4311	32.8688	39.0884	7.8610e-016	0.4519
VisuShrink (ST)	798.4422	88.7546	32.9812	38.9843	7.7354e-016	0.4522
VisuShrink (SST)	743.9543	88.4643	32.9991	37.9090	7.2653e-016	0.4521
SureShrink	716.6344	87.9920	32.8978	38.3025	2.4005e-015	0.4520
NormalShrink	732.2345	88.5233	33.3124	36.8464	6.7354e-016	0.4576
BayesShrink	724.0867	88.9992	36.8230	36.0987	1.0534e-015	0.4581
Non-log SWT	300.2841	86.3232	43.8271	11.2285	1.5783e-016	0.4577
Non-log DWT	341.3989	87.1112	39.4162	16.4850	1.0319e-015	0.4588
KalmanShrink	867.1277	90.0890	32.6884	39.0884	3.2675e-015	0.4591

Pratt's figure of merit [21], as shown in Table I.

On the other hand, all filters were implemented in MATLAB® (Mathworks, Natick, MA) on a PC with an Athlon (2.4 GHz) processor.

VI. CONCLUSION

We have presented a new speckle filter for SAR images based on wavelet denoising. In order to convert the multiplicative speckle model into an additive noise model, Argenti *et al*'s approach is applied. The simulations show that the KalmanShrink have better performance than the most commonly used filters for SAR imagery (for the studied benchmark parameters) which include statistical filters and several wavelets techniques in terms of smoothing uniform regions and preserving edges and features. The effectiveness of the technique encourages the possibility of using the approach in a number of ultrasound and radar applications. In fact, cleaner images suggest potential improvements for classification and recognition. Besides, considerably increased deflection ratio strongly indicates improvement in detection performance.

Finally, the method is computationally efficient and can significantly reduce the speckle while preserving the

resolution of the original image, and avoiding several levels of decomposition and block effect.

REFERENCES

[1] F. Abramovich and Y. Benjamini, "Adaptive thresholding of wavelet coefficients," *Comput. Statist. Data Anal.*, vol. 22, pp. 351-361, 1996.
[2] F. Abramovich, T. Sapatinas, and B. Silverman, "Wavelet thresholding via a Bayesian approach," *J. R. Stat.*, vol. 60, pp. 725-749, 1998.
[3] Z. Cai, T. H. Cheng, C. Lu, and K. R. Subramanian, "Efficient wavelet based image denoising algorithm," *Electron Lett.*, vol. 37, no. 11, pp. 683-685, May 2001.
[4] S. Chang, B. Yu, and M. Vetterli, "Adaptive wavelet thresholding for image denoising and compression," *IEEE Trans. Image Processing*, vol. 9, pp. 1532-1546, Sept. 2000.
[5] S. Chang, B. Yu, and M. Vetterli, "Spatially adaptive wavelet thresholding with context modelling for image denoising," *IEEE Trans. Image Processing*, vol. 9, pp. 1522-1531, Sept. 2000.
[6] H. Choi and R. Baraniuk, "Multiscale texture segmentation using wavelet-domain hidden Markov models," in Proc. Int. Conf. Signals, Syst., Comput., vol. 2, 1998, pp. 1692-1697.
[7] L. Sendur and I. W. Selesnick, "A bivariate shrinkage function for wavelet-based denoising," in Proc. IEEE Int. Conf. Acoust., Speech, Signal Processing (ICASSP), Orlando, May 13-17, 2002. [Online], Avalilable: http://taco.poly.edu/selesi/bishrink/icassp2002.pdf
[8] L. Sendur and I. W. Selesnick, "Bivariate shrinkage functions for wavelet-based denoising exploiting interscale dependency," *IEEE Trans. Signal Processing*, vol. 50, pp. 2744-2756, Nov. 2002.
[9] L. Sendur and I. W. Selesnick, "Bivariate shrinkage with local variance estimation," *IEEE Signal Processing Letters*, vol. 9, pp. 438-441, Dec. 2002.
[10] R. Grover Brown and P. Y.C. Hwang, *Introduction to Random Signals and Applied Kalman Filtering*, New York, John Wiley & Sons, Inc, 1992.
[11] S. Haykin, *Adaptive Filter Theory*, New Jersey, Prentice-Hall, Inc., 1991.
[12] S. Haykin, *Modern Filters*, New York, MacMillan Publishing Company, 1990.
[13] C. W. Helstrom, *Probability and Stochastic Processes for Engineers*, New York, MacMillan Publishing Company, 1991.
[14] S. M. Kay, *Fundamentals of Statistical Signal Processing: Estimation Theory*, New Jersey, Prentice-Hall, Inc., 1993.
[15] R. E. Kalman, "A new approach to linear filtering and prediction problems", J. Basic Eng., Series 82D, pp.35-45, Mar. 1960.
[16] F. Argenti and L. Alparone, "Speckle removal from SAr images in the undecimated wavelet domain," *IEEE Trans. Geosci. Remote Sensing*, vol. 40, pp. 2363-2374, Nov. 2002.
[17] H. Xie, L. E. Pierce, and F. T. Ulaby, "Statistical properties of logarithmically transformed speckle," *IEEE Trans. Geosci. Remote Sensing*, vol. 40, pp. 721-727, Mar. 2002.
[18] J. W. Goodman, "Some fundamental properties of speckle," Journal Optics Society of America, 66:1145-1150, 1976.
[19] M. Mastriani and A. Giraldez, "Enhanced Directional Smoothing Algorithm for Edge-Preserving Smoothing of Synthetic-Aperture Radar Images," *Journal of Measurement Science Review*, vol 4, no.3, pp.1-11, 2004. [Online], Available: http://www.measurement.sk/2004/S3/Mastriani.pdf
[20] H.S. Tan. (2001, October). Denoising of Noise Speckle in radar Image. [Online]. Available: http://innovexpo.itee.uq.edu.au/2001/projects/s804294/thesis.pdf
[21] Y. Yu, and S.T. Acton, "Speckle Reducing Anisotropic Diffusion," *IEEE Trans. Image Processing*, vol. 11, pp. 1260-1270, Nov. 2002.
[22] H. Guo, J.E. Odegard, M. Lang, R.A. Gopinath, I. Selesnick, and C.S. Burrus, "Speckle reduction via wavelet shrinkage with application to SAR based ATD/R," Technical Report CML TR94-02, CML, Rice University, Houston, 1994.
[23] X.-P. Zhang, "Thresholding Neural Network for Adaptive Noise reduction," *IEEE Trans. Neural Networks*, vol. 12, pp. 567-584, May 2001.
[24] D.L. Donoho and I.M. Johnstone, "Adapting to unknown smoothness via wavelet shrinkage," *Journal of the American Statistical Association*, vol. 90, no. 432, pp. 1200-1224, 1995.
[25] D.L. Donoho and I.M. Johnstone, "Ideal spatial adaptation via wavelet shrinkage," *Biometrika*, vol. 81, pp. 425-455, 1994.
[26] D.L. Donoho, I.M. Johnstone, G. Kerkyacharian, and D. Picard, "Wavelet shrinkage: asymptopia," *Journal of Royal Stat. Soc.*, vol. 57, no.2, pp. 301-369, 1995.
[27] D.L. Donoho, I.M. Johnstone, G. Kerkyacharian, and D. Picard, "Density estimation by wavelet thresholding," *Annals of Stat.*, vol. 24, pp. 508-539, 1996.
[28] D.L. Donoho, "De-Noising by soft-thresholding," *IEEE Trans. on Inf. Theory*, vol. 41, no. 3, pp. 613-627, 1995.

Prof. Mario Mastriani was born in Buenos Aires, Argentina on February 1, 1962. He is Professor of Digital Signal Processing and Digital Image Processing of National Technological University (UTN). He is working in the speckle filter of the first synthetic aperture radar (SAR) satellite of SAOCOM Mission, National Commission of Space Activities (CONAE), Buenos Aires, Argentina. He is a projects manager of the Foundation for Knowledge Development (FUNDESCO)), Buenos Aires, Argentina. He published 34 papers. He is a currently reviewer of IEEE Transactions on Neural Networks, Signal Processing Letters, Transactions on Image Processing, Transactions on Signal Processing, Communications Letters, Transactions on Geoscience and Remote Sensing, Transactions on Medical Imaging, Transactions on Biomedical Engineering, Transactions on Fuzzy Systems; and Springer-Verlag Journal of Digital Imaging.
He (M'05) became a member (M) of ENFORMATIKA in 2004, and he is a member of the International Enformatika Conference - IEC 2006. His areas of interest include Digital Signal Processing, Digital Image Processing, wavelets and Neural Networks.

Prof. Alberto E. Giraldez was born in Trelew, Chubut, Argentina on January 2, 1949. He received his B.S. degree, and Ph.D. in Physics in 1971 and 1975 respectively, from La Plata, University, Argentina. He is Professor of Electromagnetism of Buenos Aires Institute of Technology (ITBA). He is the scientific manager of the first synthetic aperture radar (SAR) satellite of SAOCOM Mission, National Commission of Space Activities (CONAE), Buenos Aires, Argentina. He published 70 papers. He was a reviewer of Radio Science (American Geophysical Union), and Annales Geophysicae (European Geophysical Society). He is the manager of the Ionosferic Laboratory (LIARA) of Argentine Navy from 1980. He is the president of the work interim group 6/8 of the International Radiocommunication Consultive Committee (IRCC) of the International Telecommunication Union (ITU) elect in 1978, and with command renovated in 1982 and 1986 for the study of "Anomalous propagation in Very High Frequency for reflections in the Ionosphere". His areas of interest include Synthetic Aperture Radar, Digital Signal Processing, Radiopropagation and Electromagnetic Compatibility, and Radar Technology.